In-Plane Free Oscillations of Suspended Chains

Roxana Alexandra PETRE

Department of Mechanics, National Science and Technology University POLITEHNICA Bucharest, Splaiul Independentei 313, 060042 Bucharest, Romania, roxana.petre@upb.ro

Mihai Valentin PREDOI *

Department of Mechanics, National Science and Technology University POLITEHNICA Bucharest, Splaiul Independentei 313, 060042 Bucharest, Romania, mihai.predoi@upb.ro

Abstract: - Chain dynamics are of particular interest in high-voltage power lines, as chain drives in cars' motors, motorcycles, maritime anchoring of ships, and even some bridge suspensions. The equilibrium and linear oscillations of a heavy, homogeneous chain made of identical rigid links, suspended between two fixed points at different heights, are investigated. The problem of the equilibrium position of each link is solved using an original algorithm based on Lagrange multipliers, being followed by some relevant numerical examples. The chain is in a gravitational field, and the kinetic energy and force function are deduced as an original compact formula, valid for any number of links. We obtained the Lagrange equations with motion constraints imposed by the fixed positions of the two ends of the chain. The free oscillations in the vertical plane passing through the hanging points are deduced, and several numerical examples are presented.

Keywords: - Multi-body dynamics, chain equilibrium, chain oscillations.

1. INTRODUCTION

The study of chain dynamics plays an important role across a variety of fields, from engineering and marine applications to natural sciences and art. In engineering and infrastructure, understanding the behavior of chains and cables under different loads is essential for designing stable, durable structures like cable-stayed and suspension bridges. The basic models are presented in ref. [1], [2]. These structures rely on cables that must withstand environmental conditions such as wind and vibrations, which can induce complex behaviors including self-contact, making it crucial to analyze their dynamics to ensure safety and performance. For instance, in ref. [3] the authors explored how wind-induced vibrations affect cables, emphasizing the need for thorough analysis to prevent structural failures. Similarly, in [4] the impact of geometric nonlinearity on the behavior of cables is studied, thus demonstrating how even slight changes in cable curvature can significantly alter their dynamic response, which is critical for bridge stability. It is known that chains and cables are fundamental components in mechanical systems like cranes, elevators, and conveyor belts, where accurate knowledge of their behavior helps optimize load distribution, reduce wear, and prevent mechanical failures. In ref. [5] Predoi et al. investigated the dynamics of elastic cables used in cranes. H. N. Arafat and A. H. Nayfeh [6] examined how primary resonance excitations can lead to unexpected vibrations in suspended cables, highlighting the importance of understanding dynamic responses to design safer and more reliable mechanical systems.In the field of marine and offshore engineering, chains are extensively used in mooring lines to anchor ships and offshore platforms. These chains and cables often experience self-contact due to currents, waves, or motion, affecting their performance and durability. Studying their dynamics allows engineers to predict how these chains will react under various sea conditions, which is vital for maintaining the stability of these structures. In ref. [7], the writhing dynamics of cables with self- contact was investigated, reinforcing how external forces, such as currents and waves, can lead to complex behaviors that impact performance, especially in mooring applications. Additionally, understanding cable dynamics is crucial in the design of subsea pipelines and communication cables, ensuring they can endure the harsh underwater environment without damage.

Beyond engineering, chain dynamics provide insights into natural phenomena. The study of wave propagation and vibration patterns in chains can provide insights into other physical systems, such as seismic waves and the behavior of flexible structures

^{*} Author to whom correspondence should be addressed

in nature. For example, studies like those in [8] and [9] modeled and analyzed the nonlinear vibrations in suspended cables, thus demonstrating how these behaviors can help understand complex wave phenomena, such as seismic activity and energy distribution in flexible structures. Additionally, chains are often used in simulations to model complex systems, aiding scientists to understand how energy disperses and how different forces interact within a medium.

The dynamics of chains extend even into art and architecture, where flexible chains and cables are used in innovative designs. Kinetic sculptures and art installations use the movement of chains to create visually striking patterns, and a deep understanding of their dynamics allows artists to achieve controlled, predictable motion. For instance, kinetic artist Alexander Calder [10] pioneered the use of mobile structures that respond to airflow, with the movement of flexible elements playing an important role in their aesthetic appeal. In modern architecture, flexible chains and cables are used to create lightweight, tension-based structures like stadium roofs and tensile pavilions, enabling architects to blend functionality with creativity.

Furthermore, the study of chain dynamics has practical benefits, such as vibration reduction and noise control. By understanding how flexible elements behave, engineers can design systems that minimize unwanted vibrations, improving comfort and safety in various applications, from vehicles to industrial machinery. Recent advancements have also explored the potential for energy harvesting from the vibrations of chains and cables, combining principles of chain dynamics with sustainable engineering to develop new ways of generating renewable energy from wind and waves. In ref. [11], are described the effects of wind-induced forces on shallow cables, offering insights into how vibrational energy could be harvested for power generation. These developments are part of a growing field where engineers are innovating ways to convert mechanical vibrations into electrical energy, improving the efficiency and sustainability of renewable energy technologies.

Previous studies, such as [9], have investigated the equilibrium position of an extensible but perfectly flexible cable, highlighting the importance of considering extensibility, due to the fact that significant differences in the cable's shape arise depending on whether it is treated as extensible or inextensible.

Overall, the diverse applications of chain dynamics highlight its significance across multiple disciplines. Whether in engineering, natural sciences, or the arts, a deeper understanding of how chains and cables interact under various forces enables the development of safer, more efficient, and more innovative solutions. By addressing complex behaviors like vibrations and self-contact, researchers and engineers can continue to push the boundaries of design and functionality.

In this paper we examine the equilibrium position and free oscillations of a heavy, homogeneous chain of *n* links, totaling a length L and suspended between two fixed points, A and B, which are positioned at the same or at different heights. The chain is subjected only to the gravitational field. The main contributions of this paper consist in: a) a validated algorithm and computer code providing the equilibrium position of the chain using the Lagrange multipliers; b) a general formula for the kinetic energy and force function for a chain made on any number of links; c) the natural modes of vibration obtained by two methods, validating the results.

The paper is organized as follows. After this introduction, section 2 briefly presents the catenary equation as being the limit case for a large number of chain links. Next, we present an algorithm that determines the chain's equilibrium position by formulating and solving the equilibrium equations with Lagrange multipliers, which minimize the position of the mass center. The resulting equations describe the chain's equilibrium by specifying the position of each link at rest. Each scenario is compared with the classical catenary solution. Section 3 focuses on the dynamics of a chain with both ends attached. We deduce general formulas for the kinetic energy and the force function, and then we employ the nonholonomic Lagrange differential equations of the second kind in two illustrative examples. Conclusions and an appendix are ending the paper.

2. EQUATIONS OF EQUILIBRIUM

2.1. The hanging cable as a limiting case of a chain

The catenary mathematical model is used for hanging cables, assuming perfect inextensibility, but no bending stiffness. The chain is inextensible, but each link is rigid, with ideal hinges between links. These differences require a detailed analysis.

The mechanical tension **T** developed in the cable at the position vector $\overline{r}(s)$ of it, defined by the arc length s along the cable, under the action of externally applied distributed forces **p**, can only be along the tangent to the cable: $T = T\overline{\tau}$ in which $\overline{\tau} = \frac{d\overline{r}}{ds} = \frac{dx}{ds}\overline{i} + \frac{dy}{ds}\overline{j} + \frac{dz}{ds}\overline{k}$ is the unit vector tangent to the curve (cable). Equilibrium of the

perfectly flexible and inextensible element of arc *ds* of the cable implies a vector equation:

$$\mathbf{T}(s+ds) - \mathbf{T}(s) + \mathbf{p}ds = \mathbf{0} , \qquad (1)$$

from which, after simplification by ds, leads to [12]:

$$\frac{d(T\overline{\tau})}{ds} + \overline{p} = 0. {2}$$

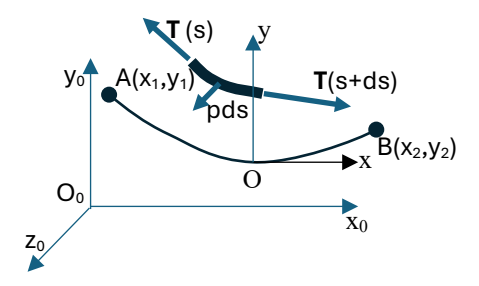


Figure 12. Element of cable at equilibrium

This differential equation can be integrated (See Appendix 1) and the equilibrium position of the heavy cable hanging in gravitational field is [12]:

$$y = a \left(ch \frac{x}{a} - 1 \right) \tag{3}$$

in a translated coordinate system with the origin O at the lowest point of the hanging cable, with $a = \frac{H}{mg}$,

m the mass per unit length, g the gravitational constant, H the horizontal component of the local tension T in the cable. If a chain of length L is suspended between two points A and B having the horizontal coordinates x_1 and x_2 , a horizontal distance d between them and a vertical distance h, then the following equations must be fulfilled:

$$\cosh \frac{x_2}{a} - \cosh \frac{x_1}{a} = \frac{h}{a}$$

$$\sinh \frac{x_2}{a} - \sinh \frac{x_1}{a} = \frac{L}{a}$$

$$x_2 - x_1 = d$$
(4)

This system of nonlinear equations yields the following nonlinear equation, which can be solved for the parameter *a* using MATLAB [13] script described in section 3.9.7 of ref. [14]:

$$\cosh\frac{d}{a} = \frac{L^2 - h^2}{2a^2} + 1.$$
(5)

In the translated reference frame with origin in O, the cable's lowest point, one end of the cable lies at $x_1 < 0$, while the other end, separated by a horizontal distance d, lies at $x_2 > 0$ and is elevated by a distance h relative to the first end. An approximate formula for the moderately tensioned catenary was deduced by Predoi et al. [15].

For a chain with many links, eq. (3) is expected to predict the link positions relatively accurately. However, in the following section, we compare the equilibrium positions of a chain having a relatively small number of links, which is a problem similar to a mechanism [16] or a simple robot [17] but with constrained motions, and prove that the similarities are valid only for a large number of links.

2.1. Equilibrium position of a hanging chain

The equilibrium position of a hanging chain with a small number of links was previously investigated by Nakagiri [18], using Lagrange multipliers and an iterative solving method. We consider also the equilibrium position as corresponding to a minimum with constraints of the mass center, but we derive a different numerical algorithm to solve the problem.

Let us consider a number of n links, each of mass m and length l. When n=2 or n=3, the static equilibrium equations for ideal rods can solve the problem, and these cases serve as validation for the current approach. On the other hand, when n is relatively large, e.g. n > 20, the catenary solution can be used to approximate the positions of the links, and this scenario also serves as a validation benchmark.

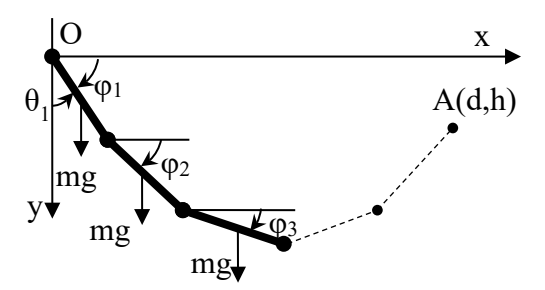


Figure 13. Configuration of three chain links

For an intermediary number n of links, we consider the notations from Figure 2, measuring each link's angle from the horizontal direction in order to simplify the comparisons with the catenary position.

The mass center of a number n of identical links, each of length l is proven to be:

$$y_c = \frac{l}{2n} \sum_{i=1}^{n} [2(n-i)+1] \sin \varphi_i$$
 (6)

This formula was obtained by complete induction starting from simple cases such as n=2, 3, 4 ...; for instance, when n=1, we obtain $y_{c1} = \frac{l \sin \varphi_1}{2}$, and so

on. A chain suspended between two fixed points O(0,0) and A(d,h) where A is horizontally displaced by d and elevated by h relative to O must comply to the following supplementary equations, representing these two conditions (Figure 2):

$$\sum_{i=1}^{n} \cos \varphi_i = \frac{d}{l}; \quad \sum_{i=1}^{n} \sin \varphi_i = \frac{h}{l}. \tag{7}$$

The static equilibrium position is minimizing the position of the mass center. The derivative of the function $\Phi(\varphi_1 \dots \varphi_n)$, which depends on the angles φ_i must cancel, accounting for the restrictions from eq. (7) using the Lagrange multipliers λ and μ [19]:

$$\Phi = \frac{l}{2n} \sum_{i=1}^{n} (2n - 2i + 1) \sin \varphi_i$$

$$-\lambda \left(\sum_{i=1}^{n} \cos \varphi_i - \frac{d}{l} \right) - \mu \left(\sum_{i=1}^{n} \sin \varphi_i - \frac{h}{l} \right)$$
(8)

The following n equations are obtained:

$$\frac{2n-2i+1}{2n}\cos\varphi_i + \lambda\sin\varphi_i - \mu\cos\varphi_i = 0, \quad i=1...n$$
 (9)

complemented by the two conditions (7) which agree with the results from ref. [18], but obtaining the solution follows a different algorithm.

The following algorithm was adopted to solve this nonlinear system of equations:

• from the last two equations of (8), that is, for i=n-1 and i=n, the following were obtained:

$$\mu = \frac{1}{2n} \frac{3\cos\varphi_{n-1}\sin\varphi_n - \cos\varphi_n\sin\varphi_{n-1}}{\sin(\varphi_n - \varphi_{n-1})}$$

$$\lambda = \frac{1}{\tan\varphi_n} \left(\mu - \frac{1}{2n}\right)$$
(10)

• the remaining *n* equations (9) were solved using our numerical solver script in MATLAB [13].

To illustrate this, we consider the chain parameters shown in Table 1, in which n represents the number of links. Since for the same n we present several geometrical configurations, the number n is repeated. These include the resulting values for the catenary a, and the end point coordinates x_1 , and x_2 , with the origin placed at the catenary's lowest point.

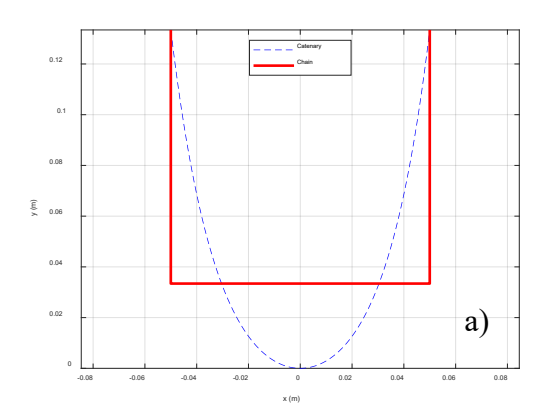
Table 3. Numerical examples of hanging chains

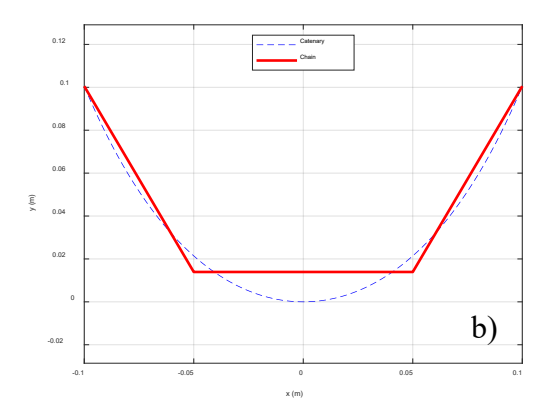
n (links)	l(m)	d(m)	h(m)	a(m)	$x_1(m)$	x2(m)
3	0.1	0.1	0	0.0176	-0.050	0.050
3	0.1	0.2	0	0.0616	-0.100	0.100
3	0.1	0.1	0.05	0.0178	-0.047	0.053
4	0.1	0.3	0	0.0178	-0.047	0.053
5	0.064	0.3	0	0.2395	-0.150	0.150
5	0.1	0.3	0.1	0.0834	-0.1331	0.1669
6	0.1	0.3	0.1	0.0697	-0.1383	0.1617

The validation examples are for 3 link chains, under different configurations: one with the distance between the suspension points equal to the link length l and another with a double distance between the

suspension points 2l (Figure 3 a, b). Both cases have the suspension points at the same height (h=0), for which the solutions can be obtained by geometrical means, without using any of the above equations.

The third example (Figure 3c) considers a height difference of l/2 between the hanging points. Although a pure geometrical solution exists and was used for validation, the usefulness of the presented algorithm will be obvious for a larger number of links.





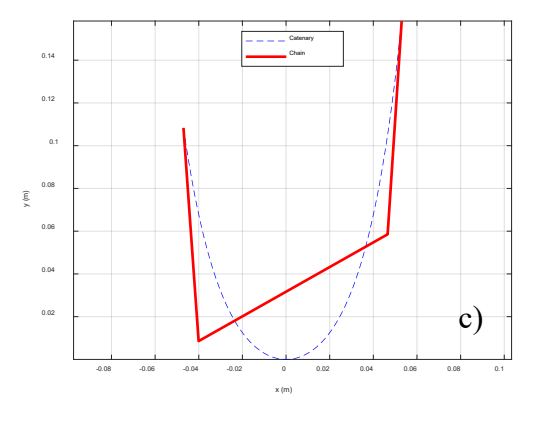


Figure 14. Equilibrium position of a simple three link chain (red) and a catenary (dashed blue) for the first three cases indicated in Table 1

More complex examples are illustrated in Figure 4, where the equilibrium positions of 4, 5, 5, and 6-link chains (shown in red) are overlaid on the catenary curve of the same length and attachment points. The example with 5 symmetric links was

introduced for comparison with ref. [18], which proves to be excellent. The efficiency of the proposed algorithm is clear, especially in cases with height differences ($h\neq 0$) between the hanging/attachment points.

As the number of links increases, it is obvious that the equilibrium positions tend to those of the catenary with the same length and suspension points. For example, in the case of 5 links with h=0 (Figure 3 b), the catenary is almost covered by the chain links.

In general, however, the existence of only an approximate overlaid of the chain links positions over the catenary proves the utility of the present study, since a cable model cannot be applied directly in such cases.

Table 4. Links angles with the vertical direction for the chain cases from Table 1.

n	θ ₁ (°)	θ2 (°)	θ ₃ (°)	θ4 (°)	θ ₅ (°)	θ ₆ (°)
3	0	90	180	-	-	-
3	30	90	150	-	-	-
3	3.98	119.97	176.31			
4	36.16	65.487	114.51	143.83	-	-
5	61.488	74.804	90.000	105.19	118.51	-
5	29.52	60.490	122.35	151.38	161.74	-
6	19.01	34.733	90.998	145.90	161.19	167.18

In the following section, some dynamic aspects of the chain behavior will be investigated, with emphasis on the free oscillations for small displacements about the equilibrium position.

The obtained angles of each link of the chain defined in Table 1, relative to the vertical direction (θ_i) are indicated in Table 2.

3. DIFFERENTIAL EQUATIONS OF MOTION IN THE VERTICAL PLANE

The chain is made of n identical links, of length l and mass m, all being in planar motion. Even if the two extreme links are rotating about fixed hinges, these extreme links can be considered to be in planar motion, from the point of view of the kinetic energy

$$E_{1} = \frac{J_{O}\dot{\theta}^{2}}{2} = \frac{1}{2} \left(J_{C}\dot{\theta}^{2} + mv_{C}^{2} \right) \text{ since } \frac{ml^{2}}{3}\dot{\theta}^{2} = m \left[\frac{l^{2}}{12}\dot{\theta}^{2} + \left(\frac{l}{2}\dot{\theta} \right)^{2} \right]$$

The kinetic energy and the force function for a serial mechanism is done in most classical textbooks of Mechanics, but in general for only two links. The classical example of Lagrange equations is applicable for serial robotic arms where one end is hinged, and the opposite end is free.

For compatibility with such existing models, the angle made by the links with the vertical direction:

 $\theta = \frac{\pi}{2} - \varphi$ (the complement angle of φ), will be used

hereafter. Also, the *Oy* axis will be directed downwards as the orientation of the gravitational force.

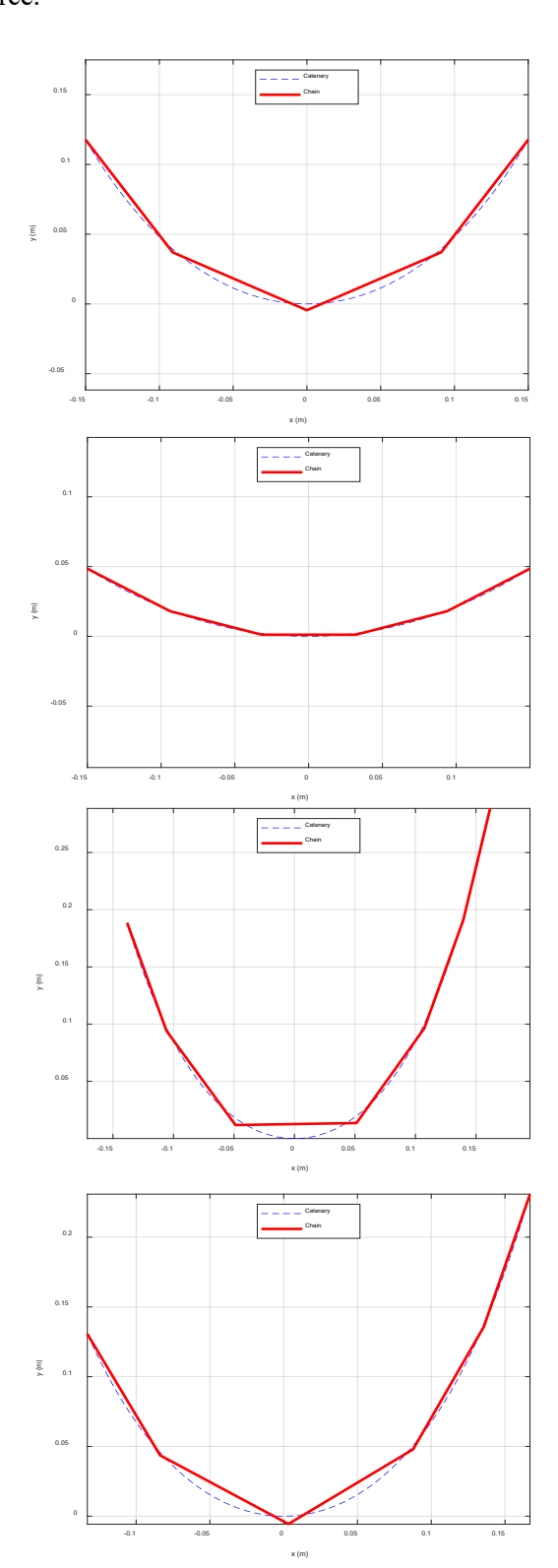


Figure 15. Equilibrium position of a chain (red) with 4, 5, and 6 links and the associated catenary (dashed blue), for the last four cases from Table 1.

We have written the kinetic energy and force function for an increasing number of chain links. The first link is hinged to a fixed hinge, then successively other links are added, each hinged to the end of the open chain.

For a chain of n links as defined in Figure 2, we have deduced by complete induction the following formulas for the kinetic energy and force function:

$$E = \frac{ml^2}{2} \left[\frac{1}{3} \sum_{i=1}^{n} \left[3(n-i) + 1 \right] \dot{\theta}_i^2 + \sum_{i=1}^{n-1} \sum_{j=i+1}^{n} \left[2(n-j) + 1 \right] \dot{\theta}_i \dot{\theta}_j \cos\left(\theta_j - \theta_i\right) \right]$$

$$U = mgl \left[\sum_{i=1}^{n} \left(n - i + \frac{1}{2} \right) \cos\theta_i \right]$$

$$(11)$$

In the force function, the angles θ_i are considered to be approximated by the static equilibrium values $\theta_{i\theta}$, negligibly affected by the small oscillations. These formulas can be used as such, in writing the Lagrange equations, but only if the last chain link (of index n) has a free end, allowing the chain to be vertical in the equilibrium position.

However, we are interested in writing the differential equations of motion for the chains with both ends attached to ideal hinges. This means that geometrical conditions expressed by equations (7) must be enforced. For small displacements, the equations (7) can be transformed into conditions for angular velocities and angular accelerations, respectively:

$$\sum_{i=1}^{n} \dot{\theta}_{i} \cos \theta_{i} = 0; \quad \sum_{i=1}^{n} \dot{\theta}_{i} \sin \theta_{i} = 0$$

$$\sum_{i=1}^{n} \ddot{\theta}_{i} \cos \theta_{i} = 0; \quad \sum_{i=1}^{n} \ddot{\theta}_{i} \sin \theta_{i} = 0$$
(12)

The Lagrange differential equations of second kind are nonholonomic:

$$\frac{d}{dt} \left(\frac{\partial E}{\partial \dot{q}_k} \right) - \frac{\partial E}{\partial q_k} = \frac{\partial U}{\partial q_k} + \lambda_1 F_1 (\dot{q}_k) + \lambda_2 F_2 (\dot{q}_k)$$

$$k = 1 \quad n$$
(13)

Another possibility is to reduce the number of independent generalized coordinates by expressing *n*-2 of them as a function of two selected generalized coordinates using the system of equations (12).

In fact, the two kinematic equations, for velocities or accelerations, reduce by 2 the number of degrees of freedom of the chain. It is obvious that the 3-link chains shown on Figure 3 have only one degree of freedom.

As an example, for a 3-link chain, with small displacements about the equilibrium position of each link, the angular velocities and accelerations of links 2 and 3 can be expressed as a function of the angular velocity and acceleration of the first link:

$$\begin{bmatrix} \dot{\theta}_{2} \\ \dot{\theta}_{3} \end{bmatrix} = \begin{bmatrix} \frac{\sin(\theta_{30} - \theta_{10})}{\sin(\theta_{20} - \theta_{30})} \\ \frac{\sin(\theta_{10} - \theta_{20})}{\sin(\theta_{20} - \theta_{30})} \end{bmatrix} \dot{\theta}_{1}$$

$$\begin{bmatrix} \ddot{\theta}_{2} \\ \ddot{\theta}_{3} \end{bmatrix} = \begin{bmatrix} \frac{\sin(\theta_{30} - \theta_{10})}{\sin(\theta_{20} - \theta_{30})} \\ \frac{\sin(\theta_{10} - \theta_{20})}{\sin(\theta_{20} - \theta_{30})} \end{bmatrix} \ddot{\theta}_{1}$$

$$(14)$$

The notations $\theta_{i\theta}$, i=1,2,3 indicate equilibrium angles, relative to which each link oscillates.

In this manner, a chain with three links is reduced to a mechanical system with one degree of freedom. This simple case will be analyzed in the following section, providing closed form solutions.

4. FREE OSCILLATIONS OF CHAINS IN THE VERTICAL PLANE

We consider in the following the particular case of a chain with 3 links, each of length l and mass m, with both ends fixed as shown in Figure 3.

The general formulas (11) that we deduced for the kinetic energy and force function for a chain with n identical links are applied in this particular case:

$$E = \frac{ml^{2}}{2} \left[\frac{7}{3} \dot{\theta}_{1}^{2} + \frac{4}{3} \dot{\theta}_{2}^{2} + \frac{1}{3} \dot{\theta}_{3}^{2} + 3 \dot{\theta}_{1} \dot{\theta}_{2} \cos(\theta_{2} - \theta_{1}) + \dot{\theta}_{1} \dot{\theta}_{3} \cos(\theta_{3} - \theta_{1}) + \dot{\theta}_{2} \dot{\theta}_{3} \cos(\theta_{3} - \theta_{2}) \right]$$

$$U = \frac{mgl}{2} \left(5 \cos\theta_{1} + 3 \cos\theta_{2} + \cos\theta_{3} \right)$$
(15)

The following notations will be used in writing the Lagrange differential equations:

$$A_{11} = \cos \theta_{10}; A_{12} = \cos \theta_{20}; A_{13} = \cos \theta_{30};$$

$$A_{21} = \sin \theta_{10}; A_{22} = \sin \theta_{20}; A_{23} = \sin \theta_{30};$$

$$C_{21} = \cos (\theta_{20} - \theta_{10}); C_{31} = \cos (\theta_{30} - \theta_{10});$$

$$C_{32} = \cos (\theta_{30} - \theta_{20}).$$
(16)

From eq. (13), one gets the nonholonomic coefficients: $A_{kj} = \frac{\partial F_k}{\partial \theta_j} \Big|_{\theta = \theta_{j0}}$ which are used in (16),

leading to the following system of differential equations:

$$\frac{7}{3}\ddot{\theta}_{1} + \frac{3}{2}C_{21}\ddot{\theta}_{2} + \frac{C_{31}}{2}\ddot{\theta}_{3} = \frac{-5}{2}\frac{g}{l}\theta_{1}\cos\theta_{10} + \lambda_{1}A_{11} + \lambda_{2}A_{21}
\frac{3}{2}C_{21}\ddot{\theta}_{1} + \frac{4}{3}\ddot{\theta}_{2} + \frac{C_{23}}{2}\ddot{\theta}_{3} = \frac{-3}{2}\frac{g}{l}\theta_{2}\cos\theta_{20} + \lambda_{1}A_{12} + \lambda_{2}A_{22}
\frac{1}{2}C_{31}\ddot{\theta}_{1} + \frac{C_{23}}{2}\ddot{\theta}_{2} + \frac{1}{3}\ddot{\theta}_{3} = \frac{-1}{2}\frac{g}{l}\theta_{3}\cos\theta_{30} + \lambda_{1}A_{13} + \lambda_{2}A_{23}
\dot{\theta}_{1}\cos\theta_{10} + \dot{\theta}_{2}\cos\theta_{20} + \dot{\theta}_{3}\cos\theta_{30} = 0
\dot{\theta}_{1}\sin\theta_{10} + \dot{\theta}_{2}\sin\theta_{20} + \dot{\theta}_{3}\sin\theta_{30} = 0$$
(17)

In fact, the last two constraints equations can be used as in eq. (14) relating two angular velocities to the third one and similar for the angular accelerations.

Case 1

As a first example, we investigate the free oscillations of the chain defined in the first row of Table 1: n=3, d=l, and h=0. Because the system consists of two rotating links and one translating link in the middle, a simple analytical solution can be obtained and used to validate the following procedure. The equilibrium position is obvious: $\theta_{10}=0$, $\theta_{20}=\pi/2$, $\theta_{30}=\pi$, with angles determined in the trigonometric positive convention. The angular velocities and accelerations are obtained using formulas (14) with the obvious case 0/0 leading to null angular velocity and acceleration, as seen from eq. (12).

$$\begin{bmatrix} \dot{\theta}_{2} \\ \dot{\theta}_{3} \end{bmatrix} = \begin{bmatrix} \frac{\sin(0)}{\sin(\pi)} \\ \frac{\sin(-\pi/2)}{\sin(\pi/2)} \end{bmatrix} \dot{\theta}_{1} = \begin{bmatrix} 0 \\ -\dot{\theta}_{1} \end{bmatrix}; \begin{bmatrix} \ddot{\theta}_{2} \\ \ddot{\theta}_{3} \end{bmatrix} = \begin{bmatrix} 0 \\ -\ddot{\theta}_{1} \end{bmatrix}$$
(18)

Using these last results, the kinetic energy and force function become:

$$E = \frac{ml^2}{2} \frac{5}{3} \dot{\theta}_1^2; \quad U = \frac{mgl}{2} (4\cos\theta_1) + Const.$$
 (19)

Assuming harmonic motion of amplitude A, angular frequency ω , initial phase β , and motion about the equilibrium position: $\theta(t) = A \exp(i\omega t + \beta)$, the angular frequency of the small amplitude oscillations in this case can be obtained:

$$\omega^2 = \frac{6}{5} \frac{g}{l} \,. \tag{20}$$

This result will be used to validate the solution obtained by Lagrange equations with constraints. The coefficients from eq. (16) in which the chain's links angles from Table 2 are injected become:

$$A_{11} = 1; A_{12} = 0; A_{13} = -1;$$

 $A_{21} = 0; A_{22} = 1; A_{23} = 0;$
 $C_{21} = 0; C_{31} = -1; C_{32} = 0.$ (21)

The differential equations are in this case:

$$(a) \frac{7}{3} \ddot{\theta}_{1} - \frac{1}{2} \ddot{\theta}_{3} = -\frac{5}{2} \frac{g}{l} \theta_{1} + \lambda_{1}$$

$$(b) \frac{4}{3} \ddot{\theta}_{2} = \lambda_{2}$$

$$(c) \frac{1}{3} \ddot{\theta}_{3} - \frac{1}{2} \ddot{\theta}_{1} = \frac{g}{2l} \theta_{3} - \lambda_{1}$$

$$(d) \dot{\theta}_{1} - \dot{\theta}_{3} = 0$$

$$(e) \dot{\theta}_{2} = 0$$

$$(22)$$

It follows from (22-d) that the angular accelerations of the first and last link are equal. Also $\ddot{\theta}_2 = \lambda_2 = 0$. From (22-a) and (22-c), λ_l can be cancelled and it will be determined: $\omega^2 = \frac{6}{5} \frac{g}{l}$, confirming the solution obtained above, using a different approach.

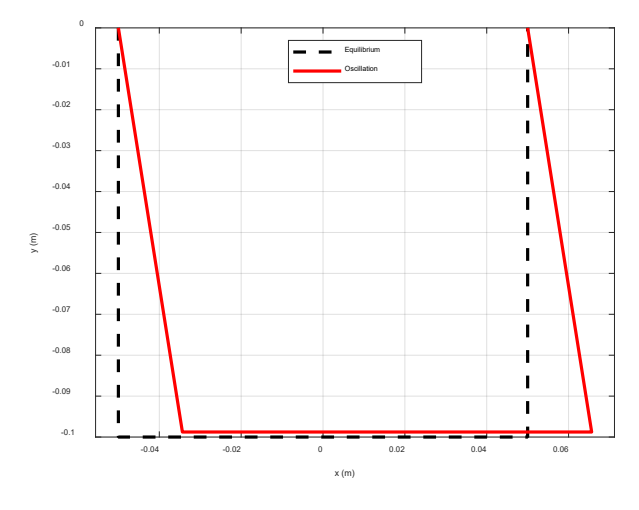


Figure 16. Free oscillations in case (1) of a three links

Case 2

The second example investigates the free oscillations of the chain defined in the second row of Table 1: n=3, d=2l, h=0, where the middle link is no longer in translation. However, an analytic solution

can be obtained by standard methods. We use the deduced algorithm for the equilibrium position: $\theta_{I0} = \pi/6$, $\theta_{20} = \pi/2$, $\theta_{30} = 5\pi/6$, with angles determined in the trigonometric positive convention. The angular velocities and accelerations are obtained using formulas (14):

$$\begin{bmatrix} \dot{\theta}_{2} \\ \dot{\theta}_{3} \end{bmatrix} = \begin{bmatrix} \frac{\sin(2\pi/3)}{\sin(-\pi/3)} \\ \frac{\sin(-\pi/3)}{\sin(-\pi/3)} \end{bmatrix} \dot{\theta}_{1} = \begin{bmatrix} -\dot{\theta}_{1} \\ \dot{\theta}_{1} \end{bmatrix}; \begin{bmatrix} \ddot{\theta}_{2} \\ \ddot{\theta}_{3} \end{bmatrix} = \begin{bmatrix} -\ddot{\theta}_{1} \\ \ddot{\theta}_{1} \end{bmatrix}$$
(23)

The kinetic energy and force function become:

$$E = \frac{ml^2}{2} \frac{3}{2} \dot{\theta}_1^2;$$

$$U = \frac{mgl}{2} \left(-2\sqrt{2} \right) \frac{\theta_1^2}{2} + C_1 \theta_1 + C_2.$$
(24)

Constant C_I is not relevant for the oscillation problem and is only contributing to the equilibrium position. The angular acceleration obtained in this case is:

$$\omega^2 = \frac{2\sqrt{3}}{3} \frac{g}{I} \,. \tag{25}$$

The second approach is to use the Lagrange equations with constraints. The coefficients from eq. (16), in which the chain's links angles from Table 2 are injected, become:

$$A_{11} = \frac{\sqrt{3}}{2}; A_{12} = 0; A_{13} = -\frac{\sqrt{3}}{2};$$

$$A_{21} = \frac{1}{2}; A_{22} = 1; A_{23} = \frac{1}{2};$$

$$C_{21} = \frac{1}{2}; C_{31} = -\frac{1}{2}; C_{32} = \frac{1}{2}.$$
(26)

The differential equations are in this case:

The differential equations are in this case.

(a)
$$\frac{7}{3}\ddot{\theta}_{1} + \frac{3}{4}\ddot{\theta}_{2} - \frac{1}{4}\ddot{\theta}_{3} = -\frac{5\sqrt{3}}{4}\frac{g}{l}\theta_{1} + \lambda_{1}\frac{\sqrt{3}}{2} + \lambda_{2}\frac{1}{2}$$

(b) $\frac{3}{4}\ddot{\theta}_{1} + \frac{4}{3}\ddot{\theta}_{2} + \frac{1}{4}\ddot{\theta}_{3} = \lambda_{2}$

(c) $-\frac{1}{4}\ddot{\theta}_{1} + \frac{1}{4}\ddot{\theta}_{2} + \frac{1}{3}\ddot{\theta}_{3} = \frac{\sqrt{3}}{4}\frac{g}{l}\theta_{3} - \lambda_{1}\frac{\sqrt{3}}{2} + \lambda_{2}\frac{1}{2}$

(d) $\frac{\sqrt{3}}{2}\dot{\theta}_{1} - \frac{\sqrt{3}}{2}\dot{\theta}_{3} = 0$

(e) $\frac{1}{2}\dot{\theta}_{1} + \dot{\theta}_{2} + \frac{1}{2}\dot{\theta}_{3} = 0$

It follows from (27-d) that near the equilibrium position, the angular velocities and accelerations of the first and third link are identical. From (27-e) the angular velocity and acceleration of the second link is equal but in opposite direction with those of the first and second link. From (27-b) can be obtained $\lambda_2 = -\frac{1}{3}\ddot{\theta}$. Summing the equations (27-a) and (27-c), one gets:

$$\frac{3}{2}\ddot{\theta}_{1} = -\sqrt{3}\frac{g}{l}\theta_{1}.$$
 (28)

Obviously, for harmonic motions, the angular frequency in this case is $\omega^2 = \frac{2\sqrt{3}}{3} \frac{g}{l}$, confirmed by formula (25), and the natural mode is shown on Figure 6.

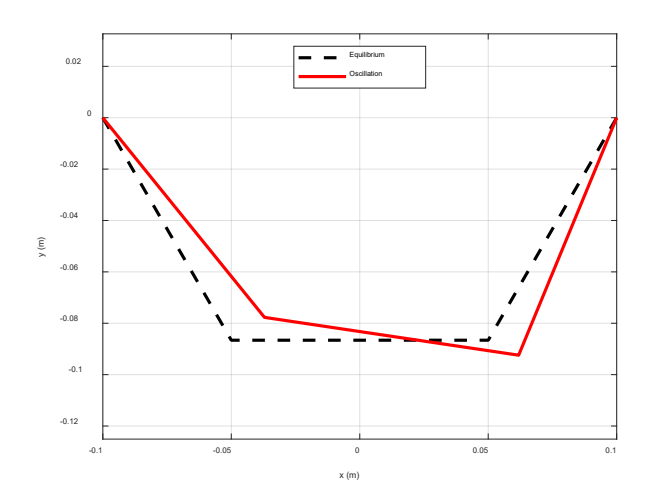


Figure 17. Free oscillations in case (2) of a three links chain.

The use of n Lagrange equations with two constraints is more general than reducing the system to one degree of freedom, preferable for chains with more links.

The two investigated cases use the same chains, only the horizontal distance between the hanging points is doubled. As a direct consequence, the non-dimensional natural frequency obtained in the first

case:
$$\Omega_1 = \omega_1 \sqrt{\frac{l}{g}} = \sqrt{\frac{6}{5}} = 1.09545$$
, is reduced in the

second case to
$$\Omega_2 = \omega_2 \sqrt{\frac{l}{g}} = \sqrt{\frac{2\sqrt{3}}{3}} = 1.07457$$
.

As is well known, a decrease in the natural frequency of a given mechanical system indicates a reduction in its mechanical stiffness. In this analysis, the reduction of stiffness in case 2 is attributed to the motion of the central link, for which the mass center is moving less than in case 1, along the vertical

direction. Moreover, while one of the lateral links raises its mass center, the other lowers it, which does not occur in the links of case 1.

5. CONCLUSIONS

The analysis of the chain's equilibrium position and small oscillations with respect to this equilibrium position is addressed in this study.

The equilibrium position of the n-link chain was obtained by an extremum with constraints equation, applied to the position of the mass center of the given chain.

A compact formula for the kinetic energy and force function for a chain with one end fixed was deduced.

The constraints introduced by fixing the other end of the chain are dealt with by reducing the number of degrees of freedom of the investigated chain by two, which is an original approach. Two cases of three-link chains are completely solved and compared with the classical approach of mechanical systems with one degree of freedom.

Other cases with a larger number of links were not investigated by the authors, considering that as the number of links increases, the existing formulas for cable vibrations become applicable.

The obtained results of this work represent the basis for further studies on chain dynamics, such as forced oscillations, inclusion of energy dissipation between the chain links. Also, the nonlinear oscillations of chains are among the perspectives.

Appendix 1

The catenary equation.

For a freely hanging cable of mass per unit length m (kg/m), attached in a gravitational field of acceleration g by points A and B situated in the vertical plane Oxy, the differential equation (2) implies two differential equations in the vertical plane:

$$\begin{cases}
\frac{d}{ds} \left(T \frac{dx}{ds} \right) = 0 \\
\frac{d}{ds} \left(T \frac{dy}{ds} \right) - mg = 0
\end{cases}$$
(A1)

The constant *H* resulting from the first differential equation represents the horizontal component of the cable's tension: $H = T \frac{dx}{ds} = T \cos \varphi$ where $\varphi(s)$ is the

local slope angle of the cable. The second differential equation becomes:

$$\frac{d}{dx}\left(H\frac{dy}{dx}\right)\frac{dx}{ds} = mg. \tag{A2}$$

In the initial $O_0x_0y_0$ plane, the elementary arc is $ds = dx\sqrt{1 + \left(\frac{dy}{dx}\right)^2}$ and equation (A2) becomes:

$$\frac{\frac{dy'}{dx}}{\sqrt{1+{y'}^2}} = \frac{mg}{H}, \text{ with the usual notation } y' = \frac{dy}{dx}.$$

Applying a change of function: $y' = \sinh(\eta)$ it follows: $\frac{dy'}{dx} = \cosh(\eta) \frac{d\eta}{dx}$. After obvious

simplifications, eq. (A2) leads to: $\frac{d\eta}{dx} = \frac{mg}{H}$, with a

general solution
$$\eta = \frac{mg}{H}x + C_1$$
, or

$$y' = \sinh\left(\frac{mg}{H}x + C_1\right)$$
. Integrating this last resulting

function, the general solution of the suspended cable in the gravitational field can be obtained:

$$y = \frac{H}{mg} \cosh\left(\frac{mg}{H}x + C_1\right) + C_2. \tag{A3}$$

Translating the system of axes with the origin O in the lowest point of the hanging cable, the boundary conditions, in this system of axes are: x = 0; y = 0; y' = 0, the equilibrium equation becomes the classical common catenary static equilibrium curve for a heavy cable: $y = a\left(ch\frac{x}{a}-1\right)$, with $a = \frac{H}{mg}$, describing a

constant depending on the mechanical tension in the cable.

REFERENCES

- Irvine, M. H., Cable structures; Cambridge, Mass., MIT Press, United States of America, 1981.
- [2] Oproescu, G., *Dinamica firelor. Modelare si Experiment.*; Bucharest, Romania, Ed. Impuls, 2015.
- [3] I. Golebiowska, I.; Peszynski, K., Cable vibration caused by wind, EPJ Web of Conferences, 2018, Vol. 180, pp. 1-6, DOI:10.1051/epjconf/201818002031.
- [4] Mansour, A.; Mekki, O.B.; Montassar, S.; Rega, G., Catenary-induced geometric nonlinearity effects on cable linear vibrations, *Journal of Sound and Vibration*, 2018, Vol. 413, pp. 332-353, DOI: 10.1016/j.jsv.2017.10.012.

- [5] Predoi, M.V.; Enescu, N.; Ceauşu, V.; Ion. C.; Motomancea, A., Un model mecanic privind dinamica firelor elastice, *Buletinul Universității Petrol-Gaze, Seria Tehnică*, 2000, Vol.52, Issue 2, pp.63-66.
- [6] Arafat, H.N.; Nayfeh, A.H., Non-Linear Responses of Suspended Cables to Primary Resonance Excitations, *Journal of Sound and Vibration*, 2003, Vol. 266, Issue 2, pp. 325-356, DOI: 10.1016/S0022-460X(02)01393-7.
- [7] Goyal, S.; Perkins, N.C.; Lee, C.L., Writhing Dynamics of Cables with Self-contact, *International Journal of Non-Linear Mechanics*, 2008, Vol. 43, Issue 1, pp. 65-73, DOI: 10.1016/j.ijnonlinmec.2007.10.004.
- [8] Rega, G., Nonlinear vibrations of suspended cables-Part I: Modeling and analysis, *Applied Mechanics Reviews*, 2004, Vol. 57, No. 6, pp. 443-478, DOI: 10.1115/1.1777224.
- [9] Rega, G., Nonlinear vibrations of suspended cables—Part II: Deterministic phenomena, *Applied Mechanics Reviews*, 2004, Vol. 57, No. 6, pp. 479-514, DOI: 10.1115/1.1777224.
- [10] Art in context-since 1995. Available online: https://artincontext.org/mobile-by-alexander-calder/ (accessed on 25 January 2025).
- [11] Zuli, D.; Picardo, G.; Luongo, A., On the Nonlinear Effects of the Mean Wind Force on the Galloping Onset in Shallow Cables, *Nonlinear Dynamics*, 2021, Vol. 103, pp. 1059-1066, DOI: 10.1007/s11071-020-05886-y.

- [12] Bratu P., Mecanica Teoretică, Bucharest, Romania, Ed. Impuls, 2006.
- [13] MathWorks Inc., MATLAB (R2022b); Natick, Massachusetts, United States of America, 2022.
- [14] Predoi, M.V., *Problems in Technical Mechanics*, *Vol. 1*; Bucharest, Romania, MatrixRom, 2023.
- [15] Predoi, M.V.; Bugaru, M.; Motomancea, A.; Dragomirescu, C., O generalizare a formei de echilibru a firului greu, *Buletinul Universității Petrol-Gaze*, 1999, vol. 51, No. 1, pp. 223-228.
- [16] Nguyen, T.V.; Petre, R.A.; Stroe, I., Application of Lagrange Equations for Calculus of Internal Forces in a Mechanism, U.P.B. Sci. Bull., series D, 2016, Vol. 78, Issue 4, pp. 15-26.
- [17] Mare, I.C.; Negrean, I.; Crişan, A., Polynomial Functions in Robot Dynamics, *Romanian Journal of Acoustics and Vibration*, 2024, Vol. 20, Issue 1, pp. 91-102.
- [18] Nakagiri, S., A note on possible natural frequencies of inplane swing of a sagging chain consisting of rigid links, Seisan-Kenkyu, 2000, Vol. 52, no. 4, pp. 27-30.
- [19] P. Lucht, "The Method of Lagrange Multipliers," Rimrock Digital Technology, Salt Lake City, 2016